PRAMANA
— journal of
physics

Vol. 86, No. 6
June 2016
pp. 1355–1367

Ultrasonic attenuation in rare-earth monoarsenides

VYOMA BHALLA[1,2,*], DEVRAJ SINGH[2], S K JAIN[3] and RAJ KUMAR[4]

[1]Amity Institute of Applied Sciences, Amity University, Noida 201 303, India
[2]Department of Applied Physics, Amity School of Engineering and Technology, Bijwasan, New Delhi 110 061, India
[3]Department of Applied Sciences, The NORTHCAP University, Sector-234, Gurgaon 122 017, India
[4]Department of Physics, Gurgaon Institute of Technology and Management, Gurgaon 122 413, India
*Corresponding author. E-mail: bhallavyoma@gmail.com

MS received 22 December 2014; revised 28 April 2015; accepted 30 July 2015
DOI: 10.1007/s12043-015-1183-5; ***e*Publication:** 17 March 2016

Abstract. The present paper deals with the theoretical calculation of mechanical and thermophysical properties of rare-earth monoarsenides, XAs (X: Np, Pu, Th and U) using elastic constants as the input parameters. These second- and third-order elastic constants (SOECs and TOECs) are determined in the temperature range 100–500 K using Coulomb and Born–Mayer potential upto second nearest neighbours. In order to provide the link between mechanical and dynamical behaviour of crystals, parameters such as Young's modulus, bulk modulus, Poisson's ratio etc. are also calculated. In addition, the Cauchy relationship is obeyed by the chosen monoarsenides and are fairly anisotropic, which results in the measurement of longitudinal and shear wave velocities along ⟨1 0 0⟩, ⟨1 1 0⟩ and ⟨1 1 1⟩ directions. The toughness/fracture (G/B_T) ratio is greater than 0.60, which implies that XAs compounds are brittle at room temperature. Further, the Debye temperature is computed using Debye average velocity as the input parameter. It helps in the characterization of lattice vibrations of a solid. In this work, ultrasonic attenuation due to phonon–phonon interaction $(\alpha/f^2)_{p-p}$ and thermoelastic loss $(\alpha/f^2)_{th}$ are computed for XAs from 100 to 500 K using Mason's theory. It further helps in evaluating the microstructural properties of the chosen materials. The obtained results indicate that XAs is mechanically stable and are compared with data available in the literature.

Keywords. Monoarsenides; Cauchy relation; anisotropy; Debye temperature; ultrasonic attenuation.

PACS Nos 43.35.+d; 62.80.+f; 62.20.dq

1. Introduction

The study of structural, electronic, magnetic and mechanical properties of rare-earth materials has become quite interesting in recent years due to their many industrial, geophysical and technological applications. These properties have been investigated to understand the role of 5f electrons under applied pressure. The actinide compounds exhibit B_1-type

crystal structure at ambient pressure. A lot of attention has been given during the last few years, for the sample preparation, single crystal growth and study of the actinide monoarsenides, AnAs (An: Np, Pu, Th and U) [1–8]. Several experimental and theoretical studies have been undertaken to determine the structural, mechanical and elastic properties of rare-earth monoarsenides [9–14]. Gerward *et al* [15] measured the structural properties of ThAs using synchrotron X-ray diffraction at high pressure. Petit *et al* [16] investigated the electronic structure of plutonium compounds. Aldred *et al* [17] attempted the study of magnetic properties of neptunium monopnictides to characterize and understand actinide magnetism. Jha *et al* [18] investigated the structural phase transition and elastic properties using a two-body interionic potential approach. Arya *et al* [19] investigated the structural phase transition and higher-order elastic constants of actinide monoarsenides using a two-body interaction potential with modified ionic charge. To the best of our knowledge, no experimental or theoretical study is available in the existing literature on temperature-dependent ultrasonic properties except a few studies on structural and elastic properties. The investigators have performed the pressure-dependent study using different models for the calculation of elastic properties. On these grounds, we have chosen monoarsenides for ultrasonic non-destructive evaluation (NDE). The temperature dependence study of actinide monoarsenides which helps in revealing the nature of bonding, thermophysical, elastoacoustic and mechanical properties of these compounds have been done. The present work represents a computational method to determine the elastic and ultrasonic properties of rare-earth monoarsenides in the temperature range 100–500 K using a theoretical model based on Coulomb and Born–Mayer potentials (van der Waals' forces of interaction have been neglected). Further, in order to study the internal structure and inherent properties of solids, the computation of ultrasonic attenuation is being performed. The temperature-dependent ultrasonic attenuation has been computed using Mason's theory [20]. The present approach has been successfully applied to predict the temperature-dependent behaviour of several rare-earth monopnictides [21–24].

2. Theory

The theory is organized in the following sections: In §2.1, a brief outline of methodology for calculating the elastic and mechanical properties is presented. Section 2.2 deals with the method to obtain an intuitive understanding about ultrasonic velocity, ultrasonic attenuation due to phonon–phonon interaction and thermoelastic loss.

2.1 *Second- and third-order elastic constants*

The interionic potential for an undeformed crystal is the sum of Coulomb and Born–Mayer potentials. It is used for computing SOECs and TOECs and is expressed as

$$\phi(R) = \phi(C) + \phi(B), \tag{1}$$

where $\phi(C)$ is the long-range electrostatic/Coulomb potential and $\phi(B)$ is the short-range repulsive/Born–Mayer potential given by

$$\phi(C) = \pm\left[\frac{e^2}{r_0}\right]; \quad \phi(B) = A\exp\left[\frac{-r_0}{b}\right], \tag{2}$$

where e is the electronic charge, $\pm$ sign applies to like and unlike ions, respectively, r_0 is the nearest-neighbour distance, b is the hardness parameter and A is the strength parameter [23]. Brugger [25] definition has been applied to calculate the second-order elastic constants (SOECs) and third-order elastic constants (TOECs) at absolute zero. According to Mori and Hiki [26], lattice energy changes with temperature. So, we add the vibrational energy part to static elastic constant.

$$C_{IJ}(T) = C^0_{IJ} + C^{\text{vib}}_{IJ} \quad \text{and} \quad C_{IJK}(T) = C^0_{IJK} + C^{\text{vib}}_{IJK}, \tag{3}$$

where superscript 0 denotes the static elastic constant at 0 K and vib denotes the vibrational part of the elastic constant at a particular temperature. The detailed expression for SOECs and TOECs are given in [27]. Using these elastic constants, the Young's modulus (Y), shear modulus (G) and bulk modulus (B_{T}) have been estimated theoretically using the approach employed in our previous study [23]. The parameters thus obtained are the prerequisite for material characterization.

2.2 *Ultrasonic velocity and Debye temperature*

The key parameter for ultrasonic characterization is the orientation-dependent ultrasonic wave velocities V_{L}, V_{S1} and V_{S2} propagating along $\langle 1\,0\,0\rangle$, $\langle 1\,1\,0\rangle$ and $\langle 1\,1\,1\rangle$ directions. These are obtained using the expressions given elsewhere [28]. Here, L and S correspond to the longitudinal and shear modes of propagation. The Debye temperature [29] can be calculated from the ultrasonic velocities of elastic waves. It is given by the following expression:

$$\theta_{\text{D}} = \frac{\hbar}{k_{\text{B}}}\left[\frac{3n}{4\pi} \times \frac{N_{\text{a}}\rho}{M}\right]^{1/3} V_m, \tag{4}$$

where $\hbar = h/2\pi$, h is the Planck constant, n is the number of atoms in the molecule, N_{a} is the Avogadro's number, ρ is the density, M is the molecular mass and k_{B} is the Boltzmann constant, respectively and V_m is the Debye average velocity. The Debye average velocity is given by the following expression along different crystallographic directions.

$$\begin{aligned} V_m &= \left[\frac{1}{3}\left\{\frac{1}{V_{\text{L}^3}} + \frac{2}{V_{\text{S1}^3}}\right\}\right]^{-1/3}; \text{ along } \langle 1\,0\,0\rangle \text{ and } \langle 1\,1\,1\rangle \text{ directions} \\ &= \left[\frac{1}{3}\left\{\frac{1}{V_{\text{L}^3}} + \frac{2}{V_{\text{S1}^3}} + \frac{1}{V_{\text{S2}^3}}\right\}\right]^{-1/3}; \text{ along } \langle 1\,1\,0\rangle \text{ direction.} \end{aligned} \tag{5}$$

2.3 *Theory of ultrasonic attenuation*

Major causes for ultrasonic attenuation are electron–phonon (e–p) and phonon–phonon (p–p) interactions, lattice imperfection, ferromagnetic and ferroelectric, NMR and thermal relaxation and thermoelastic loss at different temperatures. The chosen crystals are perfect, so there will be three causes of ultrasonic attenuation i.e., electron–phonon interaction at low temperature, phonon–phonon interaction and thermoelastic relaxation mechanisms at high temperature. Present study is in the 100–500 K temperature range. In this temperature range, electron–phonon interaction is absent as there is no coupling

between electrons and acoustical phonons. Thus, we have computed the ultrasonic attenuation due to phonon–phonon (p–p) interaction and thermoelastic relaxation mechanisms in the temperature range 100–500 K. Expressions for ultrasonic attenuation due to p–p interaction or Akhieser loss for longitudnal and shear modes of propagation under the Akhieser regime ($\omega\tau \ll 1$) is given by [30,31]

$$\left(\alpha/f^2\right)_{\mathrm{L}} = \frac{4\pi^2\tau_{\mathrm{th}}E_0D_{\mathrm{L}}}{2\rho V_{\mathrm{L}}^3}; \quad \left(\alpha/f^2\right)_{\mathrm{S}} = \frac{4\pi^2\tau_{\mathrm{th}}E_0D_{\mathrm{S}}}{2\rho V_{\mathrm{S}}^3}. \tag{6}$$

The expression for ultrasonic attenuation due to thermoelastic relaxation phenomenon i.e., thermoelastic loss is given by

$$\left(\alpha/f^2\right)_{\mathrm{th}} = \frac{4\pi^2\langle\gamma_i^j\rangle^2\kappa T}{2\rho V_{\mathrm{L}}^5}, \tag{7}$$

where α is the ultrasonic attenuation constant, f denotes frequency of the ultrasonic wave, ρ is the density, V is the ultrasonic velocity for longitudinal and shear waves, E_0 is the thermal energy density, κ is the thermal conductivity and γ_i^j denotes Grüneisen number (i, j are the mode and direction of propagation respectively). D, the acoustic coupling constant, is the change in elastic modulus caused by the strain

$$D = 9\langle(\gamma_i^j)^2\rangle - \frac{3\langle(\gamma_i^j)^2\rangle C_{\mathrm{V}}T}{E_0} \tag{8}$$

and τ_{th} is the thermal relaxation time for the exchange of acoustic and thermal energy

$$\frac{1}{2}\tau_{\mathrm{L}} = \tau_{\mathrm{S}} = \tau_{\mathrm{th}} = \frac{3\kappa}{C_{\mathrm{V}}V_m^2}. \tag{9}$$

3. Results and discussion

3.1 *Second- and third-order elastic constants*

The SOECs and TOECs are computed in the 100–500 K temperature range using two parameters viz., lattice parameter a_0 and hardness parameter b given in table 1 for XAs. The SOECs and TOECs play important roles in explaining the interactions of ultrasonic vibration with thermal phonons, equation of state, etc. The obtained results are compared with the available experimental and theoretical data [18,19,21] in table 1. The vast difference in the present and literature values is due to the use of modified inter-ionic potential theory (including the van der Waals multipole interaction energies) at high pressure in latter which were neglected in our calculations [19].

The variations of SOECs with temperature for NpAs and UAs are shown in figure 1. It is clear from figure 1 that C_{11} and C_{44} increase linearly with the increase of temperature. The decrease of C_{12} with increasing temperature reflects the usual behaviour of the other rare-earth arsenides [23,32]. Further, figures 2a and 2b indicate the six independent TOECs computed at different temperatures. It plays a crucial role in the determination of Debye temperature, Grüneisen parameter and ultrasonic attenuation. From figure 2, one can see that the absolute values of C_{111}, C_{144} and C_{166} increase with the increase in temperature while the values of C_{112} and C_{123} decrease with temperature. C_{456} remains constant as the vibrational part vanishes.

Table 1. Lattice parameter (a_0), hardness parameter (b), elastic moduli (in GPa) for XAs (X = Np, Pu, Th and U) at room temperature.

Parameters	NpAs	PuAs	ThAs	UAs
a_0 (Å)	5.836[a]	5.856[a]	5.978[a]	5.776[a]
b (Å)	0.311	0.313	0.303	0.310
C_{11}	49.95	48.99	50.29	51.24
	115.85[b]			
	145.0[a]	134.9[a]	230.8[a]	208.2[a]
C_{12}	10.65	10.52	9.157	11.19
	47.93[a]			
C_{44}	13.04	12.88	11.62	13.63
C_S	19.65	19.23	20.57	20.03
A	0.663	0.669	0.565	0.680
ν	0.189	0.234	0.236	0.234
Y	36.58	37.33	36.18	39.24
B_T	23.74	23.34	22.87	24.54
G	15.37	15.13	14.63	15.90
G/B_T	0.648	0.648	0.639	0.648

[a]Ref. [19].
[b]Ref. [18].

3.2 *Cauchy relations*

The Cauchy relation [33] for SOECs and TOECs at 0 K is obeyed by the chosen materials.

$$C_{12}^0 = C_{44}^0; \quad C_{112}^0 = C_{166}^0; \quad C_{123}^0 = C_{144}^0 = C_{456}^0. \tag{10}$$

As we go to higher temperature, we find the deviation from Cauchy's relation for the chosen monoarsenides. The failure of the Cauchy relation at a finite temperature is due to the vibrational part of the energy as can be seen from figures 1, 2a, 2b, 3a and 3b. This shows that the dominance of ionic interaction decreases with the temperature.

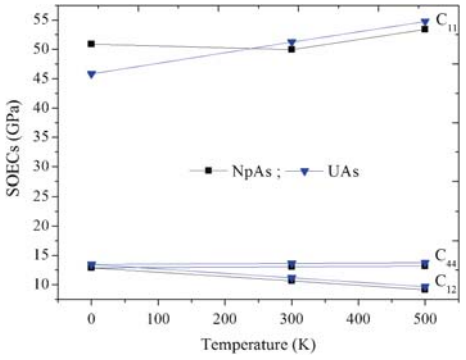

Figure 1. SOECs C_{11}, C_{12} and C_{44} for NpAs and UAs.

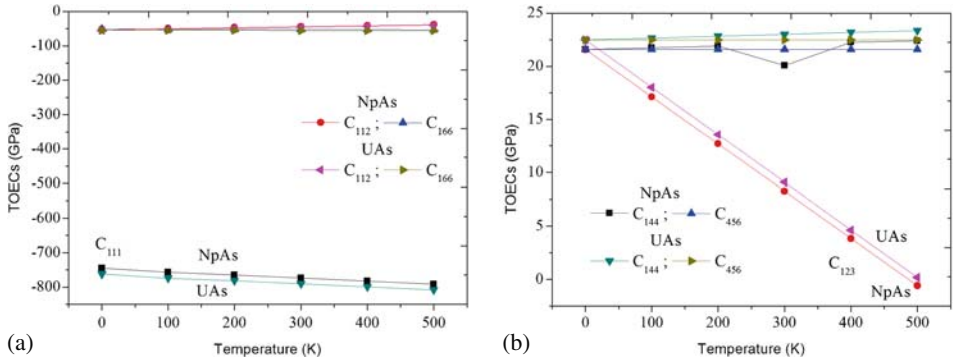

Figure 2. (**a**) TOECs C_{111}, C_{112} and C_{166} and (**b**) C_{123}, C_{144} and C_{456} for NpAs and UAs.

3.3 *Mechanical properties*

Mechanical properties are computed at room temperature and presented in table 1. The Born stability criterion, which defines the mechanical stability of a lattice, is given by

$$C_{11} + 2C_{12} > 0, \quad C_{44} > 0, \quad C_{11} - C_{12} > 0, \tag{11}$$

which are referred to as spinodal (implies bulk modulus, B_T to be positive), shear and Born criteria, respectively. From table 1, one may conclude that the chosen materials follow the Born stability criterion. Thus, these materials are mechanically stable [9,34–36]. For cubic system, the elastic anisotropy can be characterized by a Zener anisotropy ratio as suggested by Zener [37] which represents the ratio of two extreme elastic-shear coefficients:

$$A = \frac{2C_{44}}{C_{11} - C_{12}}. \tag{12}$$

From table 1, the obtained anisotropy factors, A, for XAs are not equal to 1, implying the presence of elastic anisotropy in these materials. The bulk modulus helps to obtain

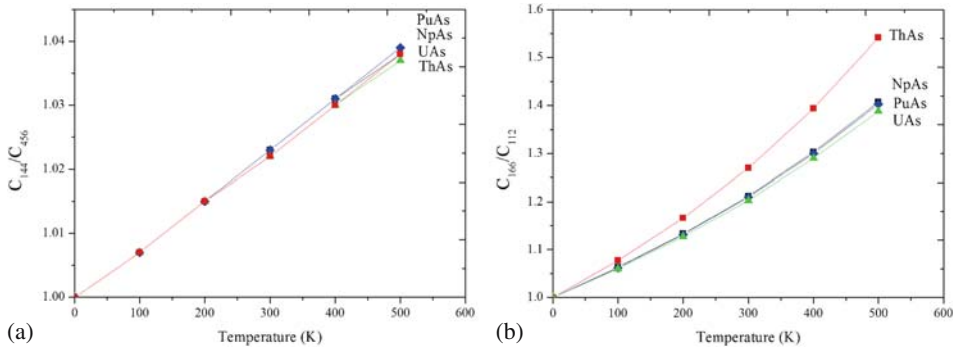

Figure 3. Graph between (**a**) C_{144}/C_{456} and (**b**) C_{166}/C_{112} vs. temperature for XAs.

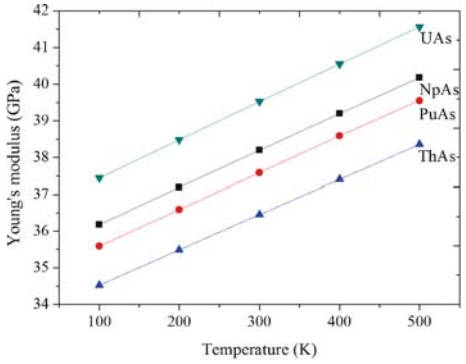

Figure 4. Young's modulus vs. temperature for XAs.

the interatomic bonding strength among the materials [38]. From table 1, the largest value of bulk modulus corresponding to the smallest lattice constant of the chosen materials is being observed. Therefore, we conclude that ThAs is harder than other chosen materials. Further, shear and tetragonal moduli C_S have been computed. They are correlated to the material hardness in a consistent manner and is found the largest for ThAs. Thus, ThAs will possess maximum resistance for deformation as compared to others. The toughness/fracture (G/B_T) ratio provides information about ionic and covalent behaviour of materials on the basis of their ductile and brittle nature respectively, in solids. The calculated values of $G/B_T \geq 0.60$ for XAs, shows the brittle (covalent) nature of these materials [39].

The Young's modulus (Y) provides the degree of stiffness i.e., higher the value of Y, the stiffer is the material [32]. In our case, we find UAs to be stiffer than the other chosen materials. The study of temperature dependence of Y is of utmost importance for studying the strength and thermal shock properties of a material. The increase in temperature causes the increase in atomic thermal vibrations which results in the change of lattice potential energy. So, the Young's modulus increases with temperature as shown in figure 4.

The value of Poisson ratio ν provides knowledge about the bonding force behaviour in solids. For central forces, the values $\nu = 0.25$ and $\nu = 0.5$ define the lower limit and upper limit, respectively. From table 1, the value of ν is $\sim$0.23 suggesting that interatomic forces in XAs are mainly non-central forces [40].

3.4 *Ultrasonic velocities and Debye temperature*

The second-order elastic constants computed for the cubic lattice of XAs along with crystal density, helps in the determination of ultrasonic velocity for longitudnal and transverse acoustic waves along the crystallographic directions $\langle 1\,0\,0\rangle$, $\langle 1\,1\,0\rangle$ and $\langle 1\,1\,1\rangle$. The computed results of ultrasonic velocities are presented in table 2. The nature and order of ultrasonic velocities are similar to other rare-earth materials like rare-earth monochalcogenides [22], praseodymium monopnictides [23] and californium monopnictides [24].

It is obvious from table 2 that the ultrasonic longitudnal wave velocity is the highest for ThAs along $\langle 1\,0\,0\rangle$ and the lowest for shear wave velocity along $\langle 1\,0\,0\rangle$ at room temperature. The Debye average velocity is the highest for ThAs along $\langle 1\,1\,1\rangle$ direction as shown in

Table 2. Temperature dependent ultrasonic velocities (in 10^3 m/s) of rare-earth monoarsenides along ⟨1 0 0⟩, ⟨1 1 0⟩ and ⟨1 1 1⟩ directions.

Materials	Directions		100 K	200 K	300 K	400 K	500 K
NpAs	⟨1 0 0⟩	V_L	2.115	2.151	2.189	2.227	2.264
		$V_{S1} = V_{S2}^{*a}$	1.114	1.116	1.118	1.120	1.123
	⟨1 1 1⟩	V_L	1.980	1.983	1.986	1.990	1.994
		$V_{S1} = V_{S2}^{*b}$	1.231	1.262	1.294	1.324	1.355
	⟨1 1 0⟩	V_L	2.015	2.026	2.039	2.052	2.065
		V_{S1}^{*c}	1.114	1.116	1.118	1.120	1.123
		V_{S2}^{*d}	1.819	1.880	1.942	2.002	2.060
PuAs	⟨1 0 0⟩	V_L	2.082	2.118	2.155	2.192	2.229
		$V_{S1} = V_{S2}$	1.100	1.102	1.105	1.107	1.109
	⟨1 1 1⟩	V_L	1.954	1.956	1.960	1.963	1.967
		$V_{S1} = V_{S2}$	1.212	1.243	1.274	1.304	1.334
	⟨1 1 0⟩	V_L	1.986	1.998	2.010	2.023	2.036
		V_{S1}	1.100	1.102	1.105	1.107	1.109
		V_{S3}	1.788	1.849	1.909	1.969	2.027
ThAs	⟨1 0 0⟩	V_L	2.216	2.255	2.296	2.336	2.376
		$V_{S1} = V_{S2}$	1.099	1.101	1.103	1.105	1.107
	⟨1 1 1⟩	V_L	1.999	2.001	2.005	2.008	2.012
		$V_{S1} = V_{S2}$	1.290	1.324	1.357	1.390	1.423
	⟨1 1 0⟩	V_L	2.055	2.068	2.081	2.095	2.109
		V_{S1}	1.099	1.101	1.103	1.105	1.107
		V_{S2}	1.946	2.011	2.076	2.140	2.202
UAs	⟨1 0 0⟩	V_L	2.107	2.143	2.180	2.217	2.253
		$V_{S1} = V_{S2}$	1.119	1.121	1.124	1.126	1.128
	⟨1 1 1⟩	V_L	1.984	1.986	1.990	1.993	1.997
		$V_{S1} = V_{S2}$	1.226	1.257	1.288	1.318	1.348
	⟨1 1 0⟩	V_L	2.015	2.027	2.039	2.052	2.064
		V_{S1}	1.119	1.121	1.124	1.126	1.128
		V_{S2}	1.806	1.866	1.927	1.986	2.044

[a]Wave polarized along ⟨1 0 0⟩ direction.
[b]Shear wave polarized along ⟨$\bar{1}$ 1 0⟩ direction.
[c]Shear wave polarized along ⟨0 0 1⟩ direction.
[d]Shear wave polarized along ⟨1 $\bar{1}$ 0⟩ direction.

figure 5. Thus, ultrasonic wave propagation along ⟨1 1 1⟩ direction will be prevailing over other directions. These directions will also play significant roles in the crystallographic studies of ThAs. The Debye temperature θ_D is evaluated using eq. (4) and is presented in figure 6. The Debye temperature is an important property for characterizing lattice vibration of solid and is affected by Debye average velocity V_m computed using eq. (5). From figure 6, we observe that the highest value of θ_D is for ThAs along ⟨1 1 1⟩ direction. The relatively high value of Debye temperature of ThAs suggests relatively strong atomic vibrations in the lattice due to the lowest atomic weight of thorium atom. The chosen materials have been studied upto 300 K (to account for thermal stability) in the existing

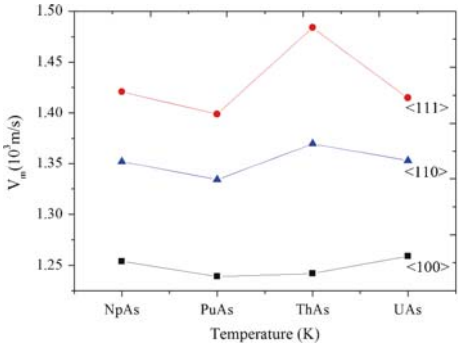

Figure 5. Debye average velocity vs. temperature along different directions for XAs.

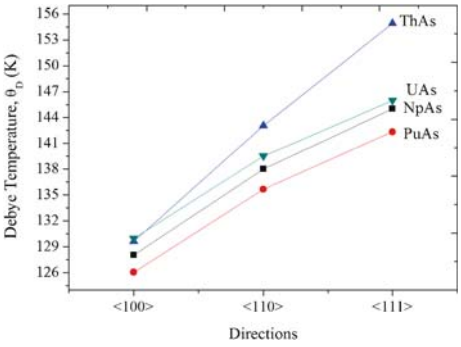

Figure 6. Debye temperature along different directions for XAs at room temperature.

literature [4,41–43]. It helps further in the determination of energy density and specific heat per unit volume which in turn is used to find attenuation.

3.5 *Acoustic coupling constants and ultrasonic attenuation*

The specific heat per unit volume (C_V) and crystal energy density (E_0) have been computed from θ_D/T tables of AIP Handbook [44] using the calculated values of ρ and θ_D. The ratio of non-linearity constant D_L/D_S along with the thermal conductivity and thermal relaxation time is given in table 3. The acoustic coupling constants D_L and D_S (for longitudinal and shear waves) which assess the ability of thermal phonons to absorb energy from sound wave have been measured along all the crystallographic directions. The increase of D_L/D_S (along $\langle 1\,0\,0\rangle$ direction) with temperature shows that ultrasonic attenuation for longitudinal modes of propagation increases with temperature and vice versa. This type of behaviour is also observed in case of other B_1 structured materials [45]. The order of τ_{th} is of picoseconds order which shows that the chosen materials are semimetallic in nature [46].

The calculated temperature-dependent SOECs and TOECs have been used for evaluating ultrasonic attenuation along with other important parameters like thermal conductivity, thermal relaxation time and acoustic coupling constants in chosen materials. The

Table 3. Thermal conductivity (κ), thermal relaxation time (τ_{th}), ratio of acoustic coupling constant (D_L/D_S) along $\langle 1\,0\,0\rangle$, $\langle 1\,1\,0\rangle$ polarized along $\langle 0\,0\,1\rangle$, $\langle 1\,\bar{1}\,0\rangle$ and $\langle 1\,1\,1\rangle$ directions at room temperature.

Materials	κ ($Wm^{-1}K^{-1}$)	τ_{th} (ps)	D_L/D_S $\langle 1\,0\,0\rangle$	D_L/D_{S1} $\langle 1\,1\,0\rangle$	D_L/D_{S2} $\langle 1\,1\,0\rangle$	D_L/D_S $\langle 1\,1\,1\rangle$
NpAs	4.06	7.29	7.807	6.794	4.509	4.827
PuAs	3.95	7.42	7.751	6.767	4.534	4.848
ThAs	4.20	7.74	8.826	7.287	4.117	4.476
UAs	4.13	7.23	7.661	6.724	4.579	4.886

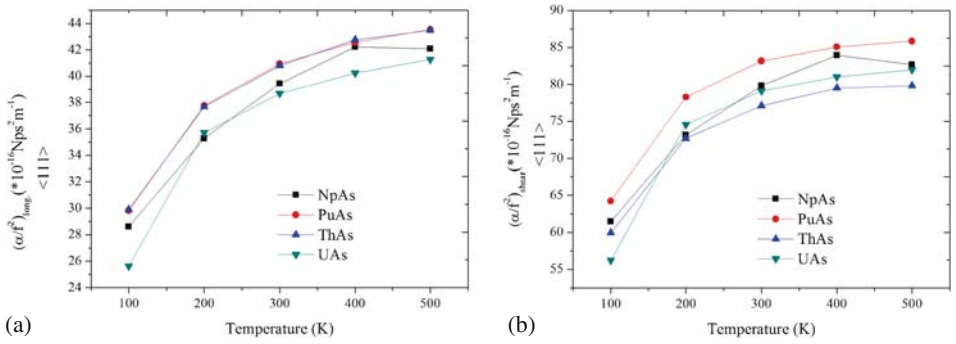

Figure 7. Temperature dependence of (**a**) longitudinal and (**b**) shear attenuation in XAs along $\langle 1\,1\,1\rangle$ direction.

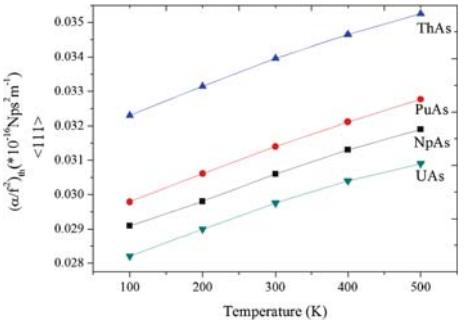

Figure 8. Debye average velocity vs. temperature along different directions for XAs.

ultrasonic attenuation due to phonon–phonon interaction $(\alpha/f^2)_{p-p}$ and thermoelastic attenuation $(\alpha/f^2)_{th}$ are computed using eqs (6)–(9) for the temperature range 100–500 K along $\langle 1\,0\,0\rangle$, $\langle 1\,1\,0\rangle$ and $\langle 1\,1\,1\rangle$ directions. The highest value of Debye average velocity and thus, the Debye temperature are obtained along $\langle 1\,1\,1\rangle$ direction as compared to $\langle 1\,0\,0\rangle$ and $\langle 1\,1\,0\rangle$ directions. Figures 7a and 7b show $(\alpha/f^2)_{long}$ and $(\alpha/f^2)_{shear}$ variation with temperature along $\langle 1\,1\,1\rangle$ direction for XAs. Along this direction, the ultrasonic attenuation

increases with the increase in temperature and then decreases slowly after 400 K in case of NpAs [29]. The average Grüneisen number for each shear mode and direction of propagation is zero. Thus, the thermoelastic loss exists only for longitudinal waves. Figure 8 shows the variation of thermoelastic attenuation $(\alpha/f^2)_{\text{th}}$ with temperature along $\langle 1\,1\,1\rangle$ direction. The thermoelastic loss $(\alpha/f^2)_{\text{th}}$ is negligible in comparison to Akhieser loss, $(\alpha/f^2)_{\text{p-p}}$ due to the smaller values of thermal conductivity. Thus, phonon–phonon interaction (p–p) is dominant for acoustic dissipation. Figure 7b depicts that the value of Akhieser loss (ultrasonic attenuation due to p–p interaction) is the lowest for ThAs along $\langle 1\,0\,0\rangle$ direction and highest along $\langle 1\,1\,1\rangle$ direction. Thus, the polishing of single crystal of ThAs is appropriate along $\langle 1\,0\,0\rangle$ for minimum attenuation of ultrasonic waves [47]. Hence the industrial applicability of ThAs is more than the others.

4. Conclusions

A simple computational approach for evaluating elastic and mechanical properties of rare-earth monoarsenides is presented. The SOECs and TOECs have been evaluated using Coulomb and Born–Mayer potentials in the temperature range of 100–500 K. The obtained results are compared with the data available in literature. Since 5f electrons become more localized on moving across the actinide series, the properties of these materials are found to be analogous to rare-earth (4f) compounds. The highest value of SOECs are found to be 51.244 GPa at room temperature for UAs. Thus, UAs is the most suitable material for mechanical purposes. The conditions $B_{\text{T}} > 0$, $C_{44} > 0$ and $C_{12} < B_{\text{T}} < C_{11}$ are satisfied by XAs and thus these materials are mechanically stable. These materials are found to be brittle in nature. Ultrasonic velocity helps in the anisotropic characterization and is found to be highest for NpAs along $\langle 1\,0\,0\rangle$ direction at room temperature. Thus, NpAs is the most suitable material for crystallographic study. The Debye average velocity decreases with the increase in molecular weight. Ultrasonic attenuation due to phonon–phonon interaction is dominant over thermoelastic loss in these materials and is found to be lowest for ThAs. So, we can anticipate that the crystal structure for ThAs contains fewer defects than other chosen materials. On the basis of the obtained results of the present investigation, ThAs may prove to be more applicable than the other materials in this study and is therefore recommended as a suitable material for further investigation into potential industrial applications. The preliminary results obtained in the present work can be used for further experimental investigation with the pulse echo overlap (PEO) technique for ultrasonic measurements, and with conventional analytical techniques such as polarizing microscopy, X-ray diffraction (XRD), surface tension analysis, solid-state nuclear magnetic resonance (NMR), scanning electron microscopy (SEM) and transmission electron microscopy (TEM) and offers a new dimension, to further study the effect of attenuation on the grain size, edge and screw dislocations, etc., and its applications.

Acknowledgements

The authors are thankful to reviewers for giving valuable comments to improve the quality of the paper.

References

[1] P Burlet, S Quezel, M Kuznietz, D Bonnisseau and J R Mignod, *J. Less Common Metals* **121**, 325 (1986)
[2] D Peleg, *Research Laboratory Annual Report*, **IA-1421** (Israel Atomic Energy Commission, Israel, 1985)
[3] J C Spirlet, E Bednarczyk, C Rijkeboer, C Rizzoli and J Rebizant, *Inorg. Chim. Acta* **94**, 111 (1984)
[4] R J Lemire, *Chemical thermodynamics of neptunium and plutonium*, OECD Nuclear Energy Agency (Elsevier, Canada, 2001) Vol. 4
[5] Z Henkie and P J Markowski, *J. Crystal Growth* **41**, 303 (1977)
[6] H E Swanson, M C Morris and E H Evans, *Standard X-ray diffraction powder patterns*, National Bureau of Standards (Dept. of Commerce, United Sates, 1966)
[7] R Horyn, *J. Crystal Growth* **63**, 407 (1983)
[8] J X Boucherle, J Flouquet and C Lacroix, *Anomalous rare earth and actinides: Valence fluctuations and heavy fermions* (Elsevier, North Holland, 2013) p. 687
[9] J M Léger, I Vedel, A M Redon, J Rossat-Mignod and O Vogt, *Solid State Commun.* **66**, 1173 (2014)
[10] R Ferro, *Act. Crystallogr.* **8**, 360 (1955)
[11] R Ferro, *Act. Crystallogr.* **9**, 817 (1956)
[12] S S Dabos, C Dufour, U Benedict, J C Spirlet and M Pages, *Physica B* **144**, 79 (1986)
[13] S D Seignon, U Benedict and J C Spirlet, *J. Less Common Metals* **153**, 133 (1989)
[14] V Srivastava and S P Sanyal, *J. Alloys Compounds* **366**, 15 (2004)
[15] L Gerward, J S Olsen, U Benedict, S Dabos and J P Itie, *High Temp. High Press.* **20**, 545 (1988)
[16] L Petit, A Svane, W M Temmerman and Z Szotek, *Eur. Phys. J. B* **25**, 139 (2002)
[17] A T Aldred, B D Dunlap, A R Harvey, D J Lam, G H Landu and M H Mueller, *Phys. Rev. B* **9**, 9 (1974)
[18] P K Jha, M Aynyas and S P Sanyal, *Indian J. Pure Appl. Phys.* **42**, 112 (2004)
[19] B S Arya, M Aynyas and S P Sanyal, *J. Optoelec. Adv. Mater.* **11**, 4, 466 (2009)
[20] W P Mason and T B Bateman, *J. Acoust. Soc. Am.* **40**, 852 (1966)
[21] R K Singh, R P Singh, M P Singh and S K Chaurasia, *Acta Phys. Pol. A* **115**, 664 (2009)
[22] D Singh, D K Pandey and P K Yadawa, *Cent. Eur. J. Phys.* **7**, 198 (2009)
[23] V Bhalla, R Kumar, S Tripathy and D Singh, *Int. J. Mod. Phys. B* **27(22)**, 1350116 (2013)
[24] R Kumar, D Singh and G Mishra, *Open J. Appl. Sci.* **1**, 1 (2011)
[25] K Brugger, *Phys. Rev.* **133**, A1611 (1964)
[26] S Mori and Y Hiki, *J. Phys. Soc. Jpn* **45(5)**, 1449 (1975)
[27] P B Ghate, *Phys. Rev.* **139(5)**, A1666 (1965)
[28] D Singh, V Bhalla, R Kumar and S Tripathi, *Indian J. Pure Appl. Phys.* **53**, 169 (2015)
[29] R Singh, *Dissipation of acoustic waves in barium monochalcogenides* (INTECH Open Access Publisher, 2010)
[30] W P Mason, *Physical acoustics* (Academic Press, New York, 1965) Vol. III B
[31] D Singh, *Study of ultrasonic attenuation in condensed materials*, D.Phil Thesis (University of Allahabad, India, 2002) submitted
[32] D K Pandey, D Singh, V Bhalla, S Tripathi and R R Yadav, *Indian J. Pure Appl. Phys.* **52**, 330 (2014)
[33] C S G Cousins, *J. Phys. C* **4**, 1117 (1971)
[34] S Bhajanker, V Srivastava and S P Sanyal, *Int. J. Adv. Elec. Comp. Engg.* **2**, 261 (2014)
[35] I R Shein and A L Ivanovskii, *Solid State Sci.* **12**, 2106 (2010)
[36] F A Rough and A A Bauer, *Constitution of uranium and thorium alloys* **UC-25**, 13th Edn (Metallurgy and Ceramics, Ohio, 1958)

[37] C Zener, *Elasticity and inelasticity of metals* (University of Chicago Press, Chicago, 1948) p. 16
[38] M Gaith and I Alhayek, *Rev. Adv. Mater. Sci.* **21**, 183 (2009)
[39] S F Pugh, *Philos. Mag.* **45**, 823 (1954)
[40] J P Watt and L Peselnick, *J. Appl. Phys.* **51**, 1525 (1980)
[41] A Blaise, D Damien and W Suski, *Solid State Commun.* **37**, 659 (1981)
[42] A E Gorum, *Acta Crystallogr.* **10**, 144 (1957)
[43] A Blaise, R Troc, R Lagnier and M J Mortimer, *J. Low Temp. Phys.* **38**, 79 (1980)
[44] D E Gray, *American Institute of Physics handbook* (McGraw-Hill Book Company, Inc., New York, 1981)
[45] R K Singh, R P Singh and M P Singh, *Acoust. Soc. Am. Proc. Meetings on Acoustics* **4**, 045006 (2008)
[46] D Singh and R R Yadav, *J. Acoust. Soc. Ind.* **29**, 176 (2001)
[47] P S Spoor, *Elastic properties of novel materials using PVDF film and resonance ultrasound spectroscopy* (Pennsylvania State University, University Park, 1997)